

## 1.2.2

### Two-Dimensional X-ray Powder Diffraction (XRD<sup>2</sup>)

Two-dimensional X-ray diffraction (2DXRD or XRD<sup>2</sup>) is a new technique in the field of X-ray diffraction (XRD). XRD<sup>2</sup> is not simply a diffractometer with a two-dimensional (2D) detector. In addition to 2D detector technology, XRD<sup>2</sup> involves 2D image processing and 2D diffraction pattern manipulation and interpretation. Because of the unique nature of the data collected with a 2D detector, a completely new concept and new approach are necessary to configure the XRD<sup>2</sup> system and to understand and analyze the 2D diffraction data. In addition, the new theory should also be consistent with the conventional theory so that the 2D data can be used for conventional applications.

First, we compare conventional X-ray diffraction (XRD) and two-dimensional X-ray diffraction (XRD<sup>2</sup>). Figure 1.3 is a schematic of X-ray diffraction from a powder (polycrystalline) sample. For simplicity, it shows only two diffraction cones, one represents forward diffraction ( $2\theta < 90^\circ$ ) and one backward diffraction ( $2\theta > 90^\circ$ ). The diffraction measurement in the conventional diffractometer is confined within a plane, here referred to as the diffractometer plane. A point detector makes a  $2\theta$  scan along a detection circle. If a one-dimensional position-sensitive detector (PSD) is used in the diffractometer, it is mounted along the detection circle (i.e., diffraction plane). Since the variation of the diffraction pattern in the direction (Z) perpendicular to the diffractometer plane is not considered in the conventional diffractometer, the X-ray beam is normally extended in the Z direction (line focus). The actual diffraction pattern measured by a conventional diffractometer is an average over a range defined by beam size in the Z direction. Since the diffraction data outside of the diffractometer plane is not detected, the material structure represented by the missing diffraction data will either be ignored, or extra sample rotation and time are needed to complete the measurement.

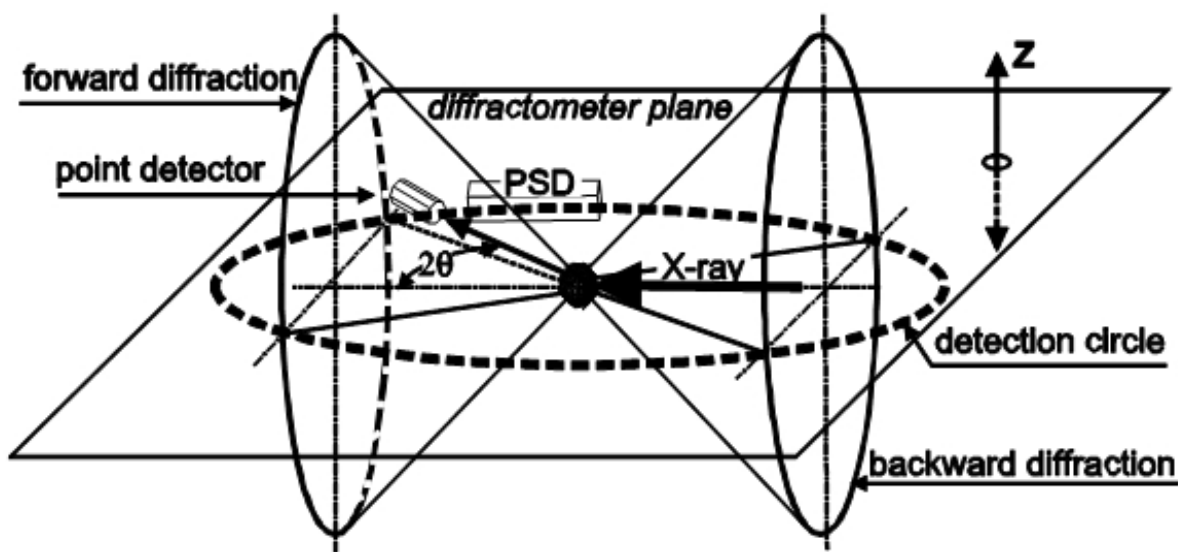


Figure 1.3 — Diffraction patterns in 3D space from a powder sample and the diffractometer plane

With a two-dimensional detector, the diffraction is no longer limited to the diffractometer plane. Depending on the detector size, distance to the sample and detector position, the whole or a large portion of the diffraction rings can be measured simultaneously. Figure 1.4 shows the diffraction pattern on a two-dimensional detector compared with the diffraction measurement range of a scintillation detector and PSD. Since the diffraction rings are measured, the variations of diffraction intensity in all directions are equally important, and the ideal shape of the X-ray beam cross-section for XRD<sup>2</sup> is a point (point focus). In practice, the beam cross-section can be either round or square in limited size.

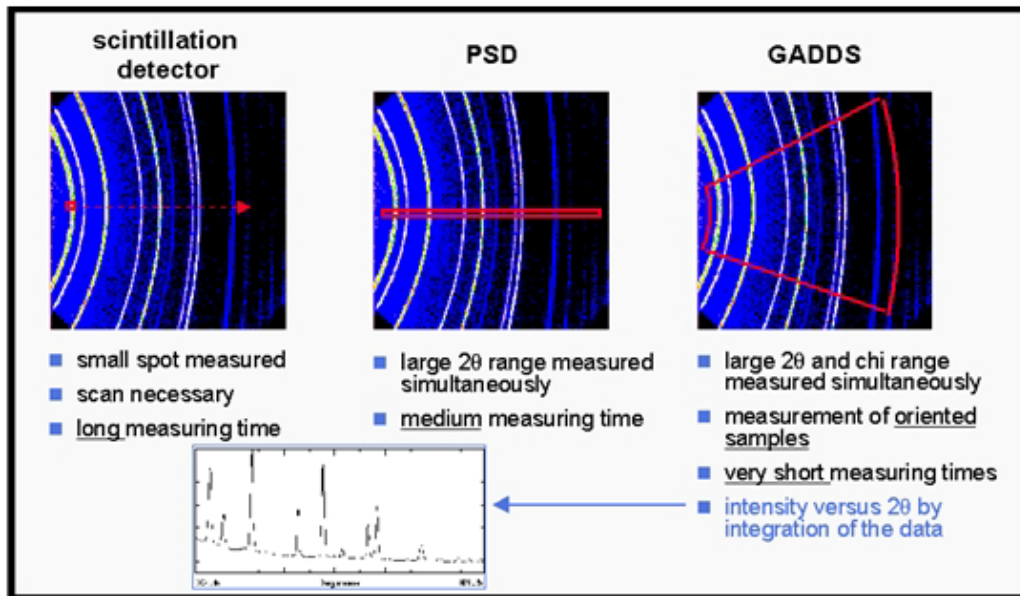


Figure 1.4 — Coverage comparison: point, line, and area detectors

## 1.3 Geometry Conventions

### 1.3.1 Diffraction Cones and Conic Sections on 2D Detectors

Figure 1.5 shows the geometry of a diffraction cone. The incident X-ray beam always lies along the rotation axis of the diffraction cone. The whole apex angle of the cone is twice the  $2\theta$  value given by the Bragg relation. The surface of the 2D detector can be considered as a plane, which intersects the diffraction cone to form a conic section.  $D$  is the distance between the sample and the detector, and  $\alpha$  is the detector swing angle, also referred to as the detector  $2\theta$  angle. The conic section takes different shapes for different  $\alpha$  angles. When imaged on-axis ( $\alpha = 0^\circ$ ), the conic sections appear as circles, producing the Debye rings familiar to most diffractionists. When the detector is at off-axis position ( $\alpha \neq 0^\circ$ ), the conic section may be an ellipse, parabola, or hyperbola. For convenience, all kinds of conic sections will be referred to as diffraction rings or Debye rings alternatively hereafter in this manual. All diffraction rings collected in a single exposure will be referred to as a frame. The area detector image (frame) is normally stored as intensity values on a  $1024 \times 1024$ -pixel grid or a  $512 \times 512$ -pixel grid.

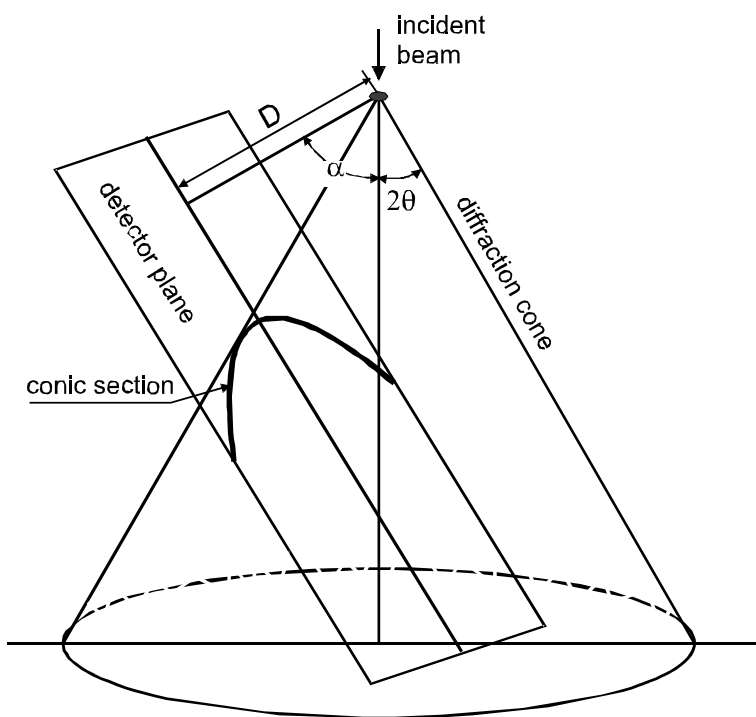


Figure 1.5 — A diffraction cone and the conic section with a 2D detector plane

### 1.3.2 Diffraction Cones and Laboratory Axes

Figure 1.6 describes the geometric definition of diffraction cones in the laboratory coordinates system,  $X_L Y_L Z_L$ .

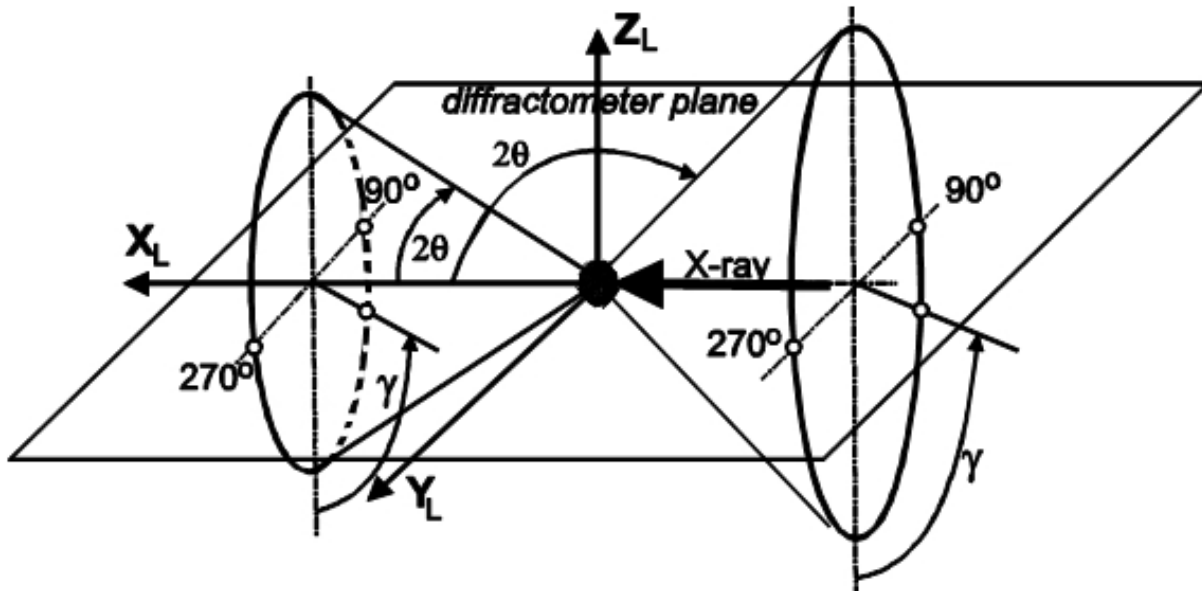


Figure 1.6 — The geometric definition of diffraction rings in laboratory axes

GADDS uses the same diffraction geometry conventions as the conventional 3-circle goniometer, which is consistent with the Bruker AXS P3 and P4 diffractometers. In these conventions, the direct X-ray beam propagates along the  $X_L$  axis,  $Z_L$  is up, and  $Y_L$  makes up a right-handed rectangular coordinate system. The axis  $X_L$  is also the rotation axis of the cones. The apex angles of the cones are determined by the  $2\theta$  values given by the Bragg equation. The apex angles are twice the  $2\theta$  values for forward reflection ( $2\theta < 90^\circ$ ) and twice the values of  $180^\circ - 2\theta$  for backward reflection ( $2\theta > 90^\circ$ ). The  $\gamma$  angle is the azimuthal angle from the origin at the 6 o'clock direction ( $-Z_L$  direction) with a right-handed rotation axis along the opposite direction of the incident beam ( $-X_L$  direction). The  $\gamma$  angle here is used to define the direction of the diffracted beam on the cone. In the past, " $\chi$ " was used to denote this angle, it was changed to  $\gamma$  to avoid confusion with the goniometer angle  $\chi$ . The  $\gamma$  angle actually defines a half plane with the  $X_L$  axis as the edge, referred to as  $\gamma$ -plane hereafter. Intersections of any diffraction cones with a  $\gamma$ -plane have the same  $\gamma$  value. The conventional diffractometer plane consists of two  $\gamma$ -planes with one  $\gamma=90^\circ$  plane in the negative  $Y_L$  side and  $\gamma=270^\circ$  plane in the positive  $Y_L$  side.  $\gamma$  and  $2\theta$  angles form a kind of spherical coordinate system which covers all the directions from the origin of sample (goniometer center). The  $\gamma$ - $2\theta$  system is fixed in the laboratory systems  $X_L Y_L Z_L$ , which is independent of the sample orientation in the goniometer. This is a very important concept when we deal with the 2D diffraction data.

As mentioned previously, the diffraction rings on a 2D detector can be any one of the four conic sections: circle, ellipse, parabola, or hyperbola. The determination of the diffracted beam direction involves the conversion of pixel information into the  $\gamma$ - $2\theta$  coordinates. In the GADDS system, the  $\gamma$  and  $2\theta$  values for each pixel are given and displayed on the frame. Users can observe all the diffraction rings in terms of  $\gamma$  and  $2\theta$  coordinates with a conic cursor, disregarding the actual shape of each diffraction ring.

### 1.3.3 Sample Orientation and Position in the Laboratory System

In the GADDS geometric convention, we use three rotation angles to describe the orientation of a sample in the diffractometer. The three angles are  $\omega$  (omega),  $\chi_g$  (goniometer chi) and  $\phi$  (phi). Since the  $\chi$  symbol has been used for the azimuthal angle on the diffraction cones in this manual, we use  $\chi_g$  to represent the  $\chi$  rotation in the 3- and 4-circle goniometer. Figure 1.7(a) shows the relationship between rotation axes ( $\omega$ ,  $\chi_g$ ,  $\phi$ ) and the laboratory system  $X_L Y_L Z_L$ .  $\omega$  is defined as a right-handed rotation about  $Z_L$  axis. The  $\omega$  axis is fixed on the laboratory coordinates.  $\chi_g$  is a left-handed rotation about a horizontal axis. The  $\chi_g$  axis makes an angle of  $\omega$  with  $X_L$  axis in the  $X_L$ - $Y_L$  plane when  $\omega \neq 0$ . The  $\chi_g$  axis lies on  $X_L$  when  $\omega$  is set at zero.  $\phi$  is a left-handed rotation. The  $\phi$  axis overlaps with the  $Z_L$  axis when  $\chi_g=0$ . The  $\phi$  axis is away from the  $Z_L$  axis by  $\chi_g$  rotation for any nonzero  $\chi_g$  angle.

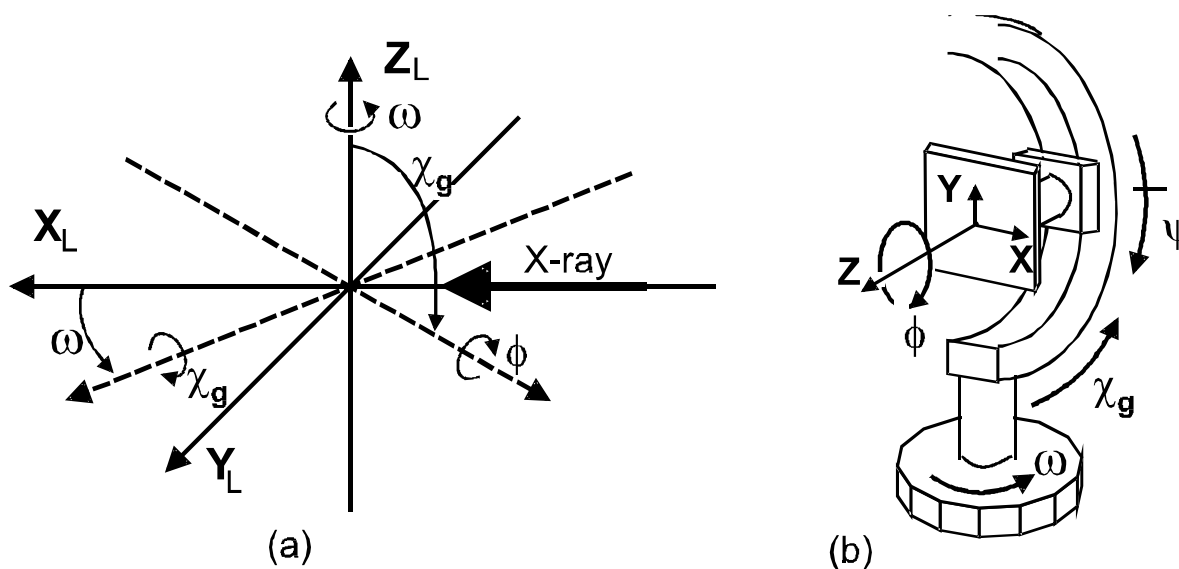


Figure 1.7 — Sample rotation and translation in the laboratory system. (a) Relationship between rotation axes and  $X_L Y_L Z_L$  coordinates; (b) Relationship among rotation axes ( $\omega$ ,  $\chi_g$ ,  $\psi$ ,  $\phi$ ) and translation axes  $XYZ$

Figure 1.7(b) shows the relationship among all rotation axes ( $\omega$ ,  $\chi_g$ ,  $\psi$ ,  $\phi$ ) and translation axes  $XYZ$ .  $\omega$  is the base rotation, all other rotations and translations are on top of this rotation. The next rotation above  $\omega$  is the  $\chi_g$  rotation.  $\psi$  is also a rotation above a horizontal axis.  $\psi$  and  $\chi_g$  have the same axis but different starting positions and rotation directions, and  $\chi_g = 90^\circ - \psi$ . In order to make the GADDS geometry definition consistent with other Bruker XRD systems, the  $\psi$  angle will be used in the later version of GADDS system. The next rotation above  $\omega$  and ( $\psi$ ) is  $\phi$  rotation. The sample translation coordinates  $XYZ$  are so defined that, when  $\omega = \chi_g = \phi = 0$ ,  $X$  is in the opposite direction of the incident X-ray beam ( $X = -X_L$ ),  $Y$  is in the opposite direction of  $Y_L$  ( $Y = -Y_L$ ), and  $Z$  overlaps with ( $Z = Z_L$ ). In GADDS, it is very common to set the  $\chi_g = 90^\circ$  ( $\psi = 0$ ) for a reflection mode diffraction as is shown in Figure 1.7(b). In this case, the relationship becomes  $X = -X_L$ ,  $Y = Z_L$ , and  $Z = Y_L$  when  $\omega = \psi = \phi = 0$ . The  $\phi$  rotation axis is always the same as the  $Z$ -axis at any sample orientation.

In an aligned diffraction system, all three rotation axes and the primary X-ray beam cross at the origin of  $X_L Y_L Z_L$  coordinates. This cross point is also known as goniometer center or instrument center. The  $X$ - $Y$  plane is normally the sample surface and  $Z$  is the sample surface normal. In a preferred embodiment,  $XYZ$  translations are above all the rotations so that the translations will not move any rotation axis away from the goniometer center. Instead, the  $XYZ$  translations bring a different part of the sample into the goniometer center. Due to this nature, if a sample is moved for the distances of  $x$  and  $y$  away from the origin in the  $X$ - $Y$  plane, the new spot on the sample exposed to the X-ray beam will be  $-x$  and  $-y$  away from the original spot.

In the past, GADDS documents and software have used the symbol  $\chi$  (or chi) for both diffraction cone and sample orientation. In this manual, we will adopt the two new symbols.  $\gamma$  (gamma) represents the direction of diffracted beam on the diffraction cone, and  $\psi$  (psi) represents a sample rotation angle. Users may see either the old or new symbol definition depending on the version of hardware or software, but can normally distinguish the two parameters from the definition if they are aware of the difference.

### 1.3.4 Detector Position in the Laboratory System

As previously mentioned, the detector position is defined by the sample-to-detector distance  $D$  and the detector swing angle  $\alpha$ . In the laboratory coordinates  $X_L Y_L Z_L$ , detectors at different positions are shown in Figure 1.8.

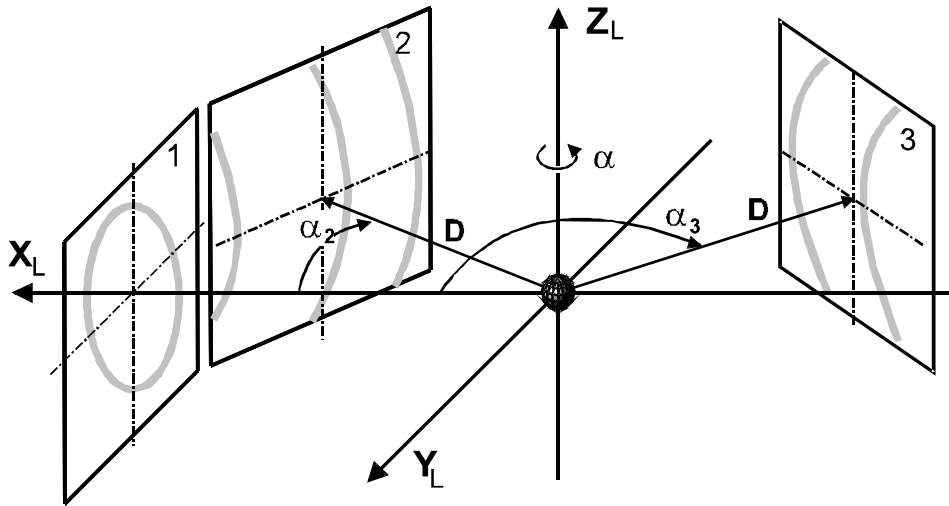


Figure 1.8 — Detector position in the laboratory system  $X_L Y_L Z_L$ :  $D$  is the sample-to-detector distance;  $\alpha$  is the swing angle of the detector

Three planes (1-3) represent the detection planes of three 2D detectors. The detector distance  $D$  is defined as the perpendicular distance from the goniometer center to the detection plane. The swing angle  $\alpha$  is a right-handed rotation angle above  $Z_L$  axis. Detector 1 is exactly centered on the positive side of  $X_L$  axis, and its swing angle is zero (on-axis). Detectors 2 and 3 are rotated away from  $X_L$  axis with negative swing angles ( $\alpha_2 < 0$  and  $\alpha_3 < 0$ ). The swing angle is sometimes called detector two-theta in GADDS documents and software. We will use  $2\theta_D$  to represent the detector swing angle hereafter in this manual. It is very important to distinguish between the Bragg angle  $2\theta$  and detector angle  $2\theta_D$ .  $2\theta$  is the measured diffraction angle on the data frame. At a given detector angle  $2\theta_D$ , a range of  $2\theta$  values can be measured. The  $2\theta$  value corresponding to the center pixel is equal to  $2\theta_D$ . Users should be able to tell the difference between two parameters although the same symbol may be used for both variables in GADDS software or documents.

## 1.4 Diffraction Data Measured by an Area Detector

Without any analysis, an area detector frame can provide a quick overview of the crystallinity, composition, and orientation of a material. If the observed Debye rings are smooth and continuous, the sample is polycrystalline and fine grained. If the rings are continuous but spotty, the material is polycrystalline and large grained (Figure 1.11). Incomplete Debye rings indicate orientation or texture (Figure 1.10). If only individual spots are observed, the material is single crystal, which can be considered the extreme case of crystallographic texture (Figure 1.9). Often, you can visually determine the number of phases when the phases have different degrees of orientation (texture).

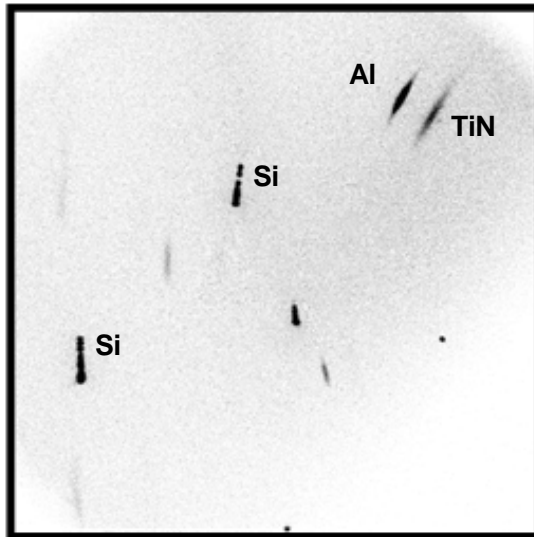


Figure 1.9 — Al TiN film on Si Specimen was rotated in  $\phi$ . Note that the Al and TiN have the same (111) orientation, and both have fiber texture. The Al and TiN are highly oriented polycrystalline materials, while the Si substrate is single crystal. The stack is roughly 0.5  $\mu\text{m}$  thick

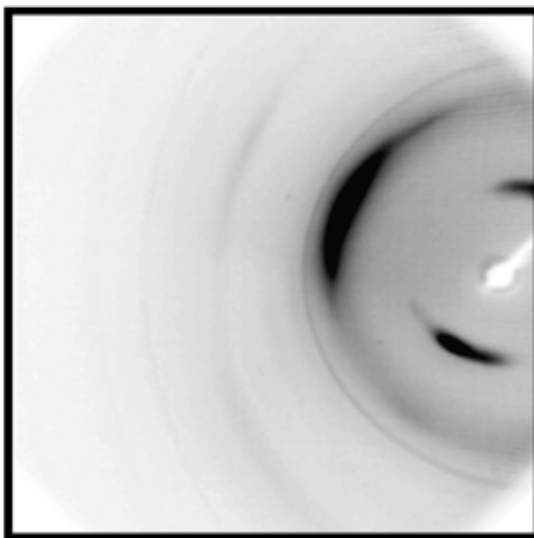


Figure 1.10 —Nylon 6 fiber with an inorganic filler. Two distinct, orthogonal orientations are visible. The faint, continuous rings are from the polycrystalline, inorganic filler

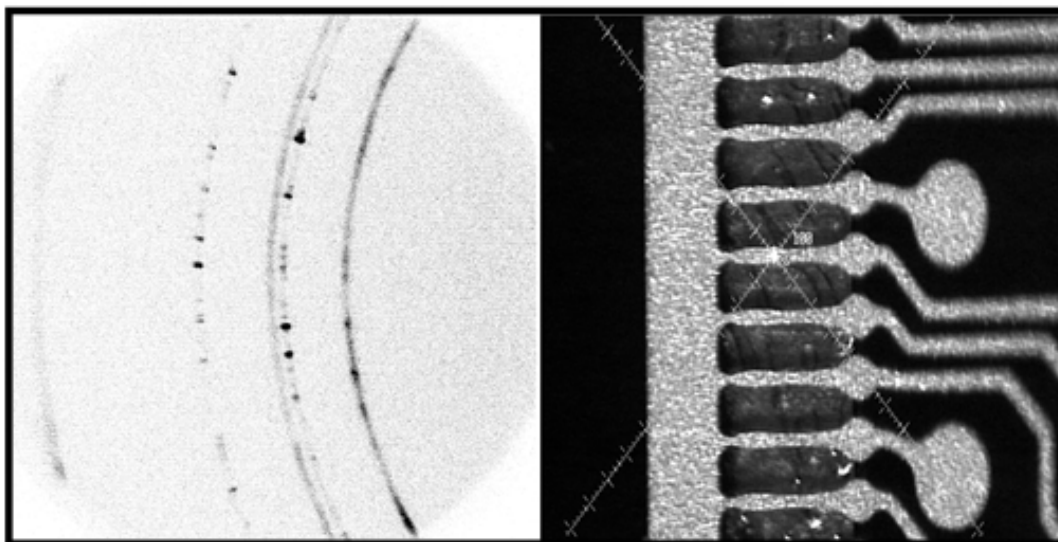


Figure 1.11 —Flexible TAB (Tape Automated Bonding) material. The two phases are gold and copper. The smooth and continuous rings are the fine-grained gold. The spotty rings belong to large-grained copper. The small divisions on the crosshair are 20  $\mu\text{m}$

When integrating an area detector frame in the  $\chi$  direction, a standard “powder pattern” (intensity versus  $2\theta$  diagram) is obtained. The added benefit of the area detector is that the intensities so obtained take preferred orientation into account. This is a tremendous advantage when performing phase analysis on oriented materials such as clay minerals. Area detector frames may also be processed to obtain texture information in the form of pole figures, fiber texture plots, and orientation indices. The coverage of the area detector frequently enables multiple poles with backgrounds to be collected simultaneously, in a small fraction of the time it takes a conventional texture diffractometer with a scintillation detector to collect a single pole.

The HI-STAR detector is a gas-filled multiwire proportional counter. It is a true photon counter, which makes it extremely sensitive for weakly diffracting materials. The extremely low background of the HISTAR makes it ideal for applications requiring “long” measurement times (tens of minutes to hours), such as small-angle X-ray scattering and microdiffraction.

## 1.5 References

1. Bob B. He, *Two-Dimensional X-Ray Diffraction*, John Wiley & Sons, 2009
1. UF Kocks, CN Tome, H.-R. Wenk, *Texture and Anisotropy*, Cambridge Univ Press, 1998
2. Philip R. Rudolf and Brian G. Landes, Two-dimensional X-ray Diffraction and Scattering of Microcrystalline and Polymeric Materials, *Spectroscopy*, 9(6), pp 22-33, July/August 1994.
3. S. N. Sulyanov, A. N. Popov and D. M. Kheiker, Using a Two-Dimensional Detector for X-ray Powder Diffractometry, *J. Appl. Cryst.* **27**, pp 934-942, 1994.
4. Hans J. Bunge and Helmut Klein, Determination of Quantitative, High-Resolution Pole-Figures with the Area Detector, *Z. Metallkd.* **87**(6), pp 465-475, 1996.